Analysis of A Larger Die, Copper Pillar Bump Flip Chip Package with No-Flow Underfill

Xiaowu Zhang [a], D. Pinjala [a], E. H. Wong [a]
[a] Institute of Microelectronics (IME), Singapore
11 Science Park Road, Singapore Science Park II, Singapore 117685
Tel: (65) 7705423; Fax: (65) 7745747; E-mail: xiaowu@ime.a-star.edu.sg

Grace Chew [b], Zhaohui Ma [b], Teck Tiong Tan [b], and Jimmy Chew [b]
[b] Advanpack Solutions Pte Ltd (APS), 54 Serangoon North Ave 4, Singapore 55584

Abstract

In the flip chip assembly process, no-flow underfill (NFU) has the advantage over traditional capillary-flow underfill because of the elimination of processing steps and the reduction of packaging cost. However, currently one of the major technical obstacles in applying no-flow underfill technology is the fillet cracking of no-flow underfill during the reflow after the moisture preconditioning. In this paper, comprehensive thermo-mechanical and hygroswelling models are established to study a larger die flip chip package with no flow underfill during reflow after moisture preconditioning. The adhesion strengths between no-flow underfill and die have been characterized. Based on the modelling results and the adhesion strength data, the reason why the crack on the no-flow underfill starts and propagates, leading to fillet cracking, is also explained. A series of parametric studies are also performed to eliminate or reduce the fillet crack. The results show that a lower coefficient of thermal expansion (CTE), a lower Young's modulus (E) and a higher cure temperature of no-flow underfill are desirable for the robustness of the package. The results also show that thinner die thickness is desirable for the robustness of the package. These findings form design guidelines for the design of larger die, copper pillar bump flip chip package with no-flow underfill.

1. Introduction

Growing demands on performance, cost and the advancement in IC technology have drastically influenced packaging and interconnnection technology. New packaging technologies and advanced materials have to be developed to handle larger dice, higher I/O counts, lower operating voltage, high power consumption and high clock frequencies [1-4]. Although ongoing research in industry addresses some of the issues, there is a deficit of work on the impact of larger die flip chip packages on package reliability. Advanpack Solutions (APS) has developed robust and wide ranging lead-free interconnect technologies for flip chip attachment of a larger die to a variety of different substrate material. The interconnection technology uses a copper pillar capped with a solder to enhance thermo-mechanical reliability [5].

No-flow underfill process has been widely accepted as a key technology to implement low-cost, high-throughput flip chip packages because of the elimination of processing steps such as flux application, flux residue cleaning, capillary underfill flow and secondary thermal curing of the underfill as shown in Figure 1 [5-18]. However, currently one of the major technical obstacles in applying no-flow underfill technology for larger dice is the fillet cracking of the no-flow underfill during the reflow (especially lead-free reflow profiles) after the moisture preconditioning

In this paper, comprehensive thermo-mechanical and hygroswelling models are established to study a larger die flip chip package with no flow underfill during reflow after moisture preconditioning. The adhesion strengths between no-flow underfill and die have been characterized. Based on the modelling results and the adhesion strength data, the reason why the crack in the no-flow underfill starts and propagates, leading to fillet cracking, is also explained. A series of parametric studies are also performed to eliminate or reduce the fillet crack. The results show that a lower coefficient of thermal expansion (CTE), a lower Young's modulus (E) and a higher cure temperature of no-flow underfill are desirable for the robustness of the package. The results also show that thinner die thickness is desirable

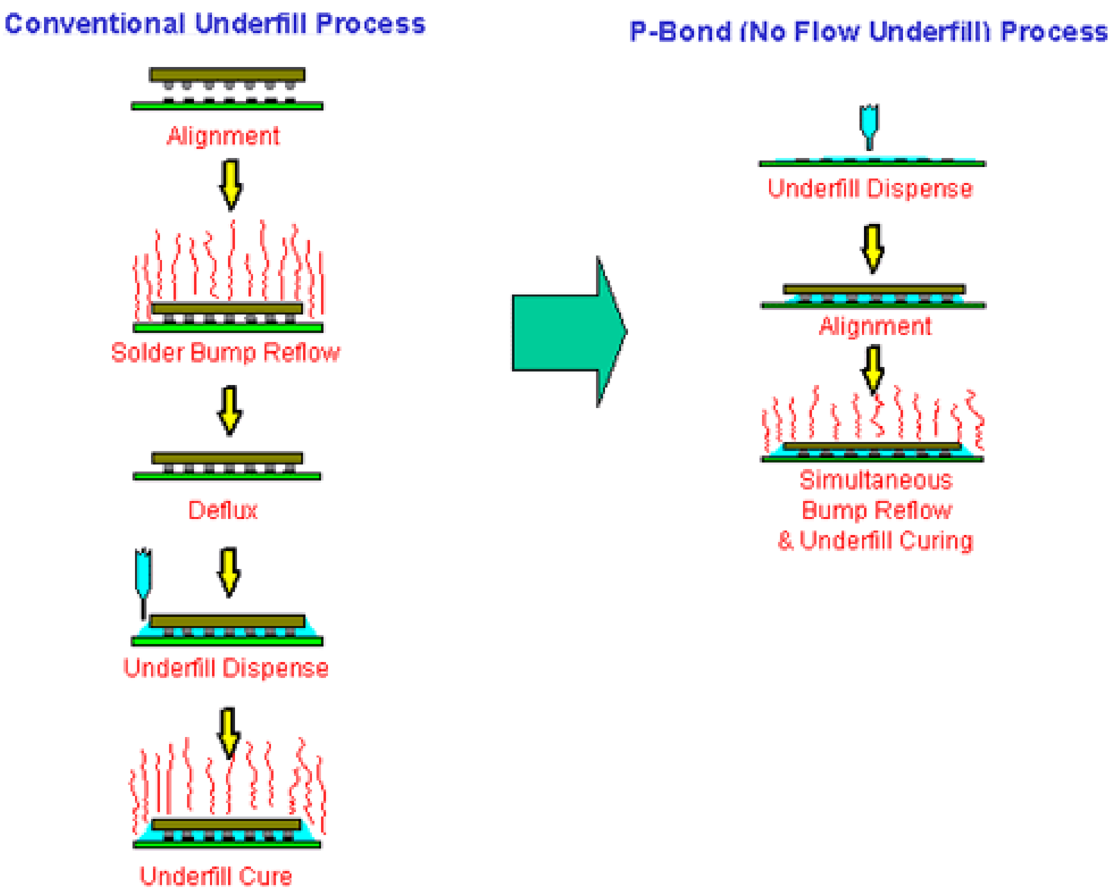

Figure 1: Conventional underfill process versus no-flow underfill.

for the robustness of the package. These findings form design guidelines for the design of larger die, copper pillar bump flip chip packages with no-flow underfill.

2. Package Description

The substrate is a laminated BGA substrate with a peripheral heat sink ring as shown in Figure 2. The substrate size is 50 mm by 50 mm. The large die size is 21.4 mm by 21.4 mm with the copper pillar bumps. The bump pitch is 200 µm. The copper pillar bumping technology uses a copper pillar capped with a solder, which was developed by APS [5]. The patented copper pillar bump for standard pitch is made up of 65 µm non-reflowable copper post capped with 35 µm pure solder (Figure 3). This unique structure ensures the copper pillar bump's distinctive advantages compared to standard eutectic or high lead solder bumps. In this paper, the number of bumps on the package is 5588. The diameter of the copper pillar is 70 µm. A cross section of the copper pillar interconnects of the package is shown in Figure 4.

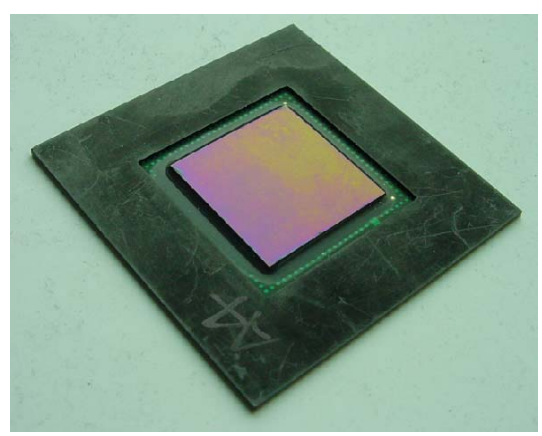

Figure 2: Outline of the larger die, copper pillar bump flip chip package with heat sink ring at the periphery.

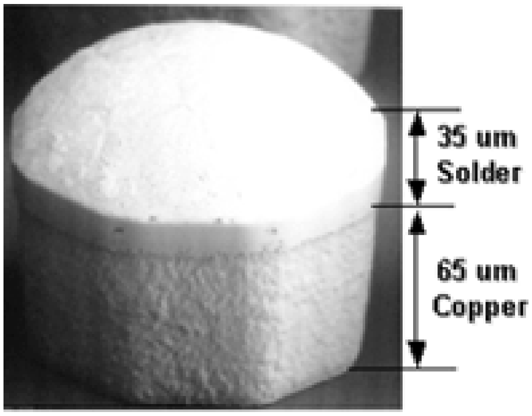

Figure 3: The copper pillar bump structure.

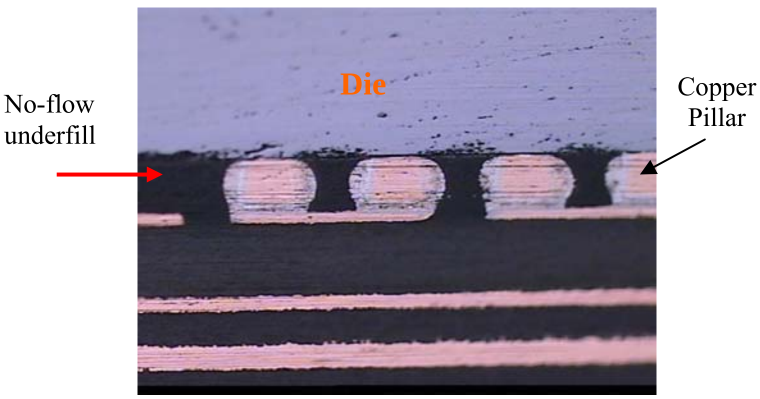

Figure 4: Cross section for one interconnect of the package.

The no-flow underfill used in this study is LR 9000 developed by APS [5]. The no-flow underfill has a high silica filler loading to solve the thermo-mechanical reliability of the large die flip chip package. The process for no-flow underfill is shown in Figure 1. First, the no-flow underfill is dispensed on the substrate. The die is then mounted on the substrate and sent for reflow attachment. During reflow attachment the no flow underfill material cures and forms the desired bond and protective layer between the die surface and substrate.

3. Material Characterization of No Flow Underfill

For the finite element modeling (FEM), proper material characterization of no flow underfill (NFU) is required. The coefficient of thermal expansion (CTE) measurement of cured NFU samples was performed using a Thermo-Mechanical Analysis (TMA) instrument. A specimen for TMA testing was prepared by placing a liquid formulation of ~4 grams into an aluminum pan (38 mm diameter). The specimen was then transferred to a preheated convective oven, and then heated to a specified temperature at about ~3ºC/min heating rate. The sample was continously cured in the oven at 150ºC for 1.5 hours to eliminate voids. After that, the sample was removed from the oven and cooled to room temperature. The aluminum pan was peeled off and the cured sample was polished into a disk with two parallel surfaces. Optical microscopy was used to detect the voids and air bubbles on the sample surfaces. A diamond saw was used to cut the polished sample into squares with dimensions of about 5x3x1 mm. After the sample was placed on the TMA sample stage, heat was applied to bring the samples from room temeperature to about 250ºC at a heating rate of 5ºC/min. The CTE was obtained by the slope of the dimensional change versus temperature curve.

The Young's modulus (E) measurement of cured NFU samples was performed using a Dynamic Mechanical Analysis (DMA) instrument. The preparation of a specimen used for the DMA test was the same as for the TMA test. But, the specimen size for DMA test was longer, at approximately 20x3x1 mm. The measurement was performed in the single cantiliver mode under 1 Hz sinusoidal strain loading. Storage modulus E′, loss modulus E″, and loss angle tanδ were calculated by the preinstalled software. The peak temperature of tanδ was defined as the DMA Tg (glass transition temperature). In this study, the Young's modulus (E) of the NFU is assumed to be equal to the storage modulus (E′) of the NFU. The CTEs, T_g and Young's modulus of the adhesive are shown in Table 1. The Poisson ratio (ν) of the NFU is equal to 0.35. Other Material Properties used in FEA are also shown in Table 1.

Moisture property characterization was done to obtain the diffusivity (D) and Saturated Moisture Concentration (Csat). D represents the rate with which moisture diffuses through a material with unit concentration gradient while Csat is defined as the maximum concentration of moisture that can be contained per volume of a material. Samples used for this characterization were blocks of dimensions 5 mm by 5 mm by 0.6 mm. Prior to moisture soaking, the samples were baked at 125°C for 24 hours to remove any moisture and residual stress. After which, the samples were soaked in a JEDEC Level 3 (30°C/60%RH) chamber until saturation. Moisture desorption of the moistured samples was then performed on a Thermogravimetric Analyzer (TGA) by holding isothermally at 30°C to measure the weight loss of the sample over a period of time. D was then extracted by fitting the experimental weight loss data to the three-dimensional diffusion equation (1) using a non-linear regression technique [18]. Csat was calculated using equation (2).

$$\frac{M_t}{M_{sat}} = 1 - \frac{512}{\pi^6}\sum_{l=0}^{\infty}\sum_{m=0}^{\infty}\sum_{n=0}^{\infty}\frac{\exp(-Dt/L_{eqv})}{(2l+1)^2 * (2m+1)^2 * (2n+1)^2}$$

$$\text{where} \quad L_{eqv} = \left[\frac{(2l+1)\pi}{x}\right]^2 + \left[\frac{(2m+1)\pi}{y}\right]^2 + \left[\frac{(2n+1)\pi}{z}\right]^2 \qquad (1)$$

x, y, z = specimen length, width and height
M_t = mass of moisture absorbed at time, t
M_{sat} = saturated mass of moisture absorbed

$$Csat = M_{sat} / volume \qquad (2)$$

Hygroscopic swelling characteriztion was done to obtain the Coefficient of Moisture Expansion (CME). A simple technique for characterization of CME was described in [18]. Samples used for this characterization were the same as for moisture diffusion characterization. Pre-test treatment was also the same. Two identical samples were baked then soaked in JEDEC Level 3 chamber until saturation. This was followed by moisture desorption at 30°C for a few hours in TMA and TGA. From TMA, change in dimension is obtained, whereas from TGA, weight loss due to moisture desorption is recorded. By plotting the strain (dimensional change) versus moisture concentration, a linear relation is obtained. This constant of linearity is the CME. The moisture properties of the NFU were obtained as following. The saturated moisture concentration (Csat) is 0.0198 mg/mm and the Coefficient of Moisture Expansion (CME) is 0.24 mm^3/mg.

4. Finite Element Model

The finite element model of the package is shown in Figure 5. The detailed finite element model for interconnect is shown in Figure 6. Material properties used in the finite element modeling are shown in Table 1. The temperature loading for the thermo-mechanical model is from the no-flow underfill curing temperature (160 ºC) to the reflow peak temperature (260 ºC).

Table 1: Material properties used in the finite element modeling.

Material	CTE1 (ppm/ºC)	CTE2 (ppm/ºC)	Elastic Modulus @25ºC (GPa)	Elastic Modulus @200ºC	Tg (ºC)	Poisson's Ratio
Substrate	19	N/A	1.7865	1.4887 GPa	N/A	0.26
No-flow underfill	37.15	117.8	5.291	1.576 MPa	107.7	0.35
Cu Pillar	17	N/A	110	N/A	N/A	0.3435
Die	2.7	N/A	120	N/A	N/A	0.28
Stiffener Ring	17	N/A	110	N/A	N/A	0.3435
Solder	22	N/A	51	37 GPa	N/A	0.3
Mold Compound	8.5	31	25	1.1 GPa	147	0.3

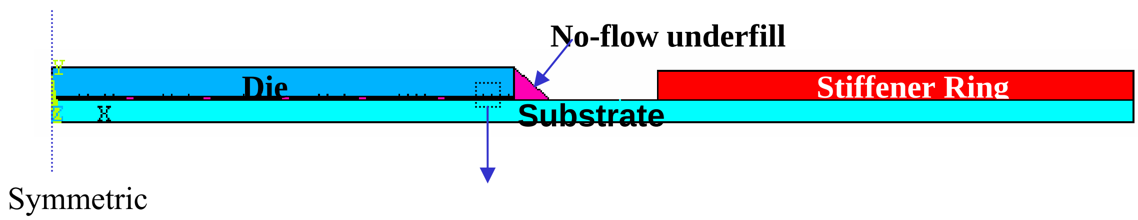

Figure 5: The finite element model of the package (die dimensions: 21.5x21.5x0.736mm; substrate thickness: 0.5mm).

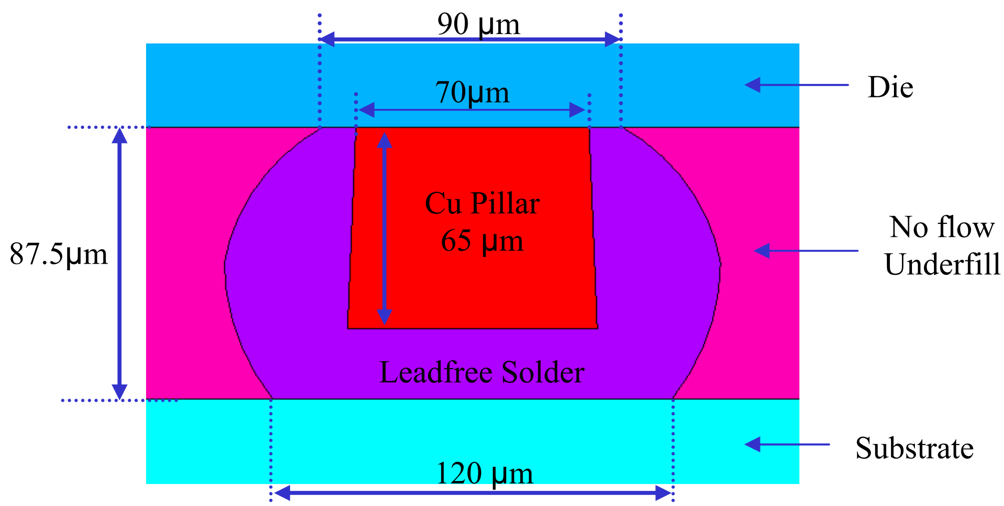

Figure 6: The detailed finite element model for a single interconnect.

The modeling consists of the following assumptions:

- The temperature change is assumed to be the same throughout the package.
- All materials are modeled as elastic materials.
- Perfect adhesion is assumed at all material interfaces.
- The package is stress free and undeformed at no-flow underfill curing temperature of 160 °C.
- The temperature loading during the reflow is from 160 °C to 260 °C.
- Moisture induced hygroscopic strain is assumed to be converted to the equivalent CTE of no-flow underfill under the same temperature loading of 160 °C to 260 °C. For example, the no-flow underfill hygrostrain is equivalent to no-flow underfill CTE of 47.52 ppm/°C under the same temperature loading of 160 °C to 260 °C using the analogous equations (3) and (4).

$$\Delta CME \times \Delta C = CTE_{eq} \times \Delta T \qquad (3)$$

$$CTE_{eq} = \frac{(0.24\ mm^3/mg) \times (0.0198\ mg/mm^3)}{260°C - 160°C} = 47.52\ (ppm/°C) \qquad (4)$$

5. Results and Discussion

Figure 7 shows thermo-mechanical shear stress in the no-flow underfill during reflow. It is found that the maximum thermo-mechanical shear stress in NFU occurs in the fillet near the die corner. The magnitude of the maximum thermo-mechanical shear stress is 21.98 MPa. Figure 8 shows hygroswelling shear stress in no-flow underfill during reflow. It is also found that the maximum hygroswelling shear stress in NFU occurs the fillet near die corner. The magnitude of the maximum hygroswelling shear stress is 8.68 MPa. Figure 9 shows superposition of thermo-mechanical stress and hygroswelling stress. The magnitude of the maximum total stress is 30.98 MPa.

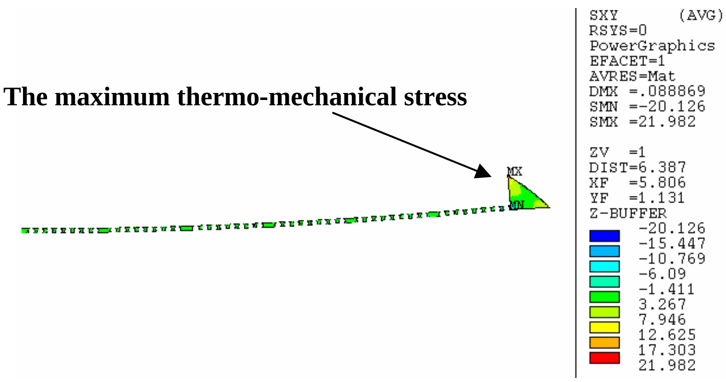

Figure 7: Thermo-mechanical stress in no-flow underfill during reflow. The maximum thermo-mechanical shear stress in NFU occurs in the fillet near the die corner.

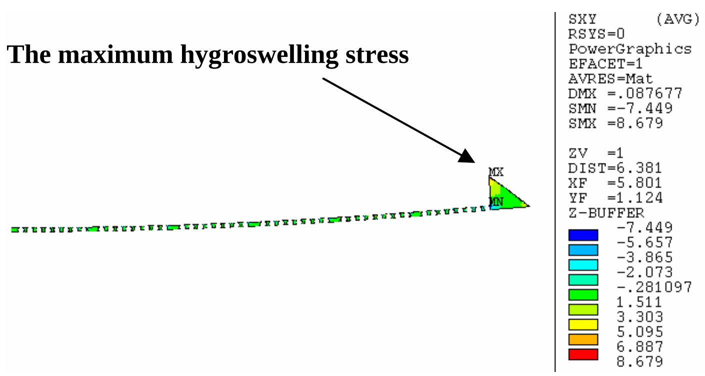

Figure 8: Hygroswelling stress in no-flow underfill during reflow. The maximum hygroswelling shear stress in NFU also occurs in the fillet near the die corner.

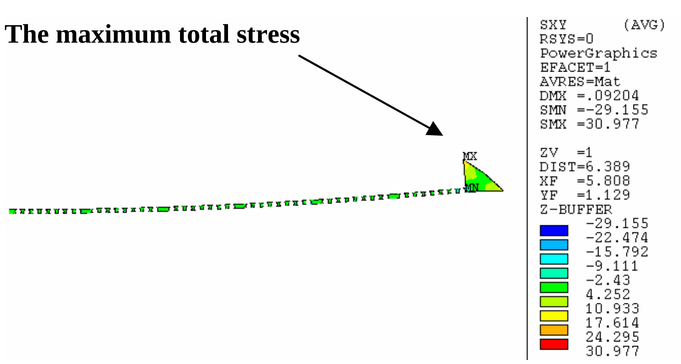

Figure 9: Superposition of thermo-mechanical stress and hygroswelling stress. The value of the total shear stress is 31 MPa.

The adhesion strength between the no-flow underfill and die has been characterized as shown in Figure 10. It is found that the room temperature adhesion strength after level-3 moisture precondition plus reflow is 29 MPa. Hence, the adhesion strength at the reflow peak temperature (260ºC) after level-3 moisture precondition plus reflow is much less than 29 MPa. The value of the total shear stress under the reflow after the moisture preconditioning is 30.98 MPa, which is much higher than the adhesion strength at reflow peak temperature (260 ºC). Thus, the crack in the no-flow underfill starts and propagates, leading to fillet cracking (Figure 11).

For parametric studies, one design variable is changed at a time with respect to the control case. The material properties for the control case are listed in Table 1. The die thickness for the control case is 0.736mm. The fillet spread for the control case is 0.8235mm. The substrate thickness for control case is 0.5mm. There are 8 effects studies relative to the control case, and results are shown in Figures 12-19. It is a comprehensive analysis on the effects of material properties of NFU, cure temperature, fillet spread, fillet height, die thickness, material properties of substrate, substrate thickness, and overmold.

The results show that a lower CTE & E of no-flow underfill and a higher cure temperature of no-flow underfill are desirable for the robustness of the package. The results also show that thinner die thickness is desirable the robustness of the package. These findings form design guidelines for the design of the larger die, copper pillar bump flip chip package with no-flow underfill.

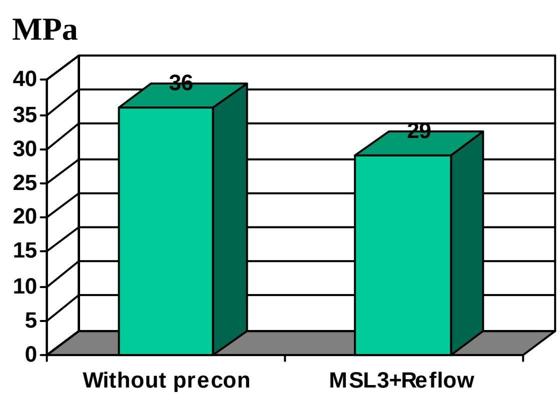

Figure 10: Adhesion strength between the no-flow underfill and the die at 25ºC.

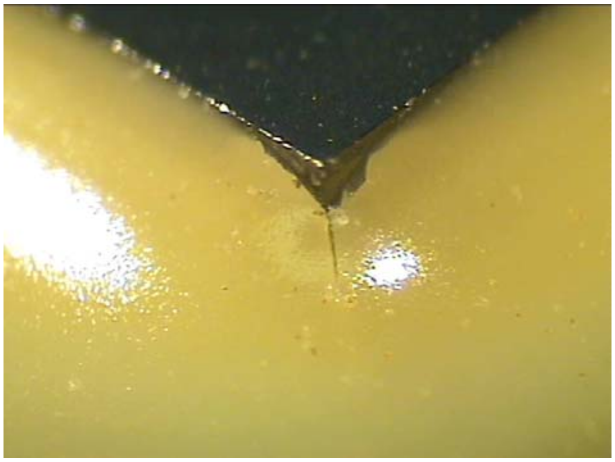

Figure 11: An example of a crack in the no-flow underfill fillet that occurs at the four corners of the die.

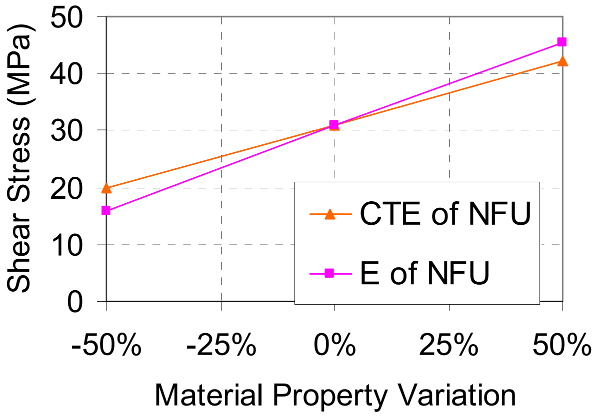

Figure 12: Effect of material properties of NFU on the total shear stress.

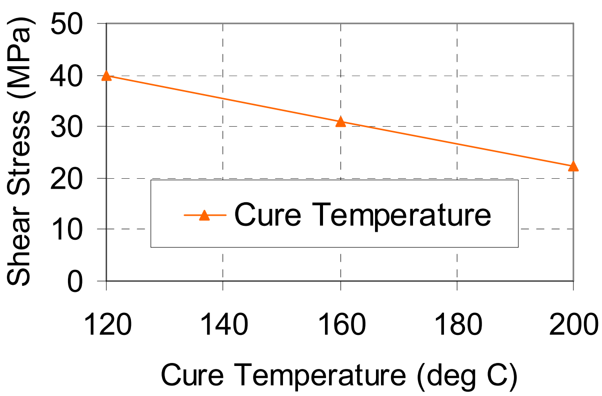

Figure 13: Effect of cure temperature on the total shear stress.

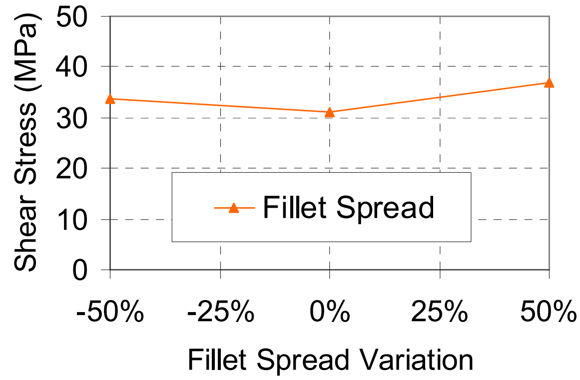

Figure 14: Effect of fillet spread on the total shear stress.

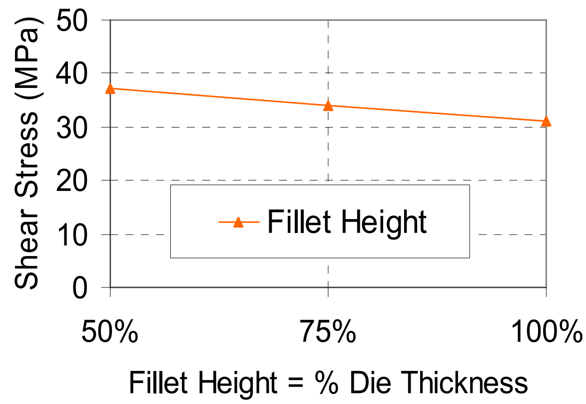

Figure 15: Effect of fillet height on the total shear stress.

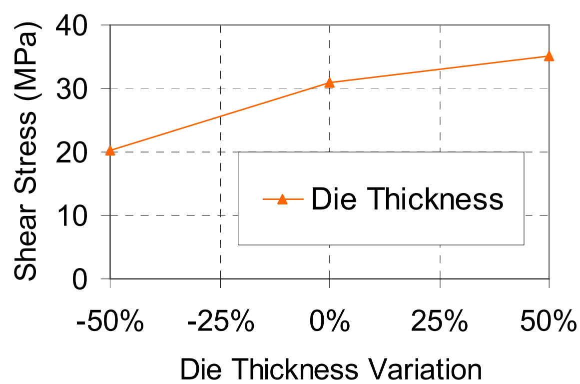

Figure 16: Effect of die thickness on the total shear stress.

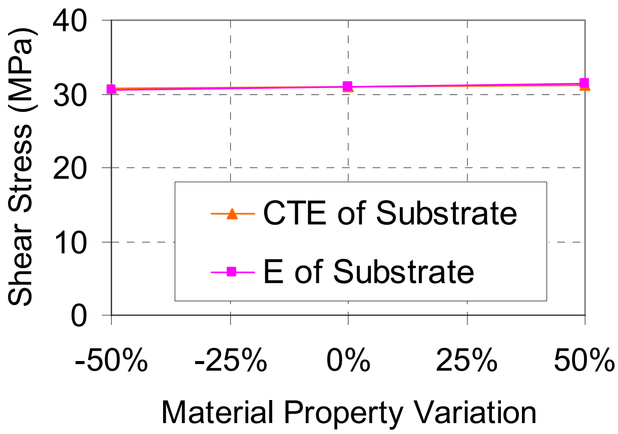

Figure 17: Effect of material properties of substrate on the total shear stress.

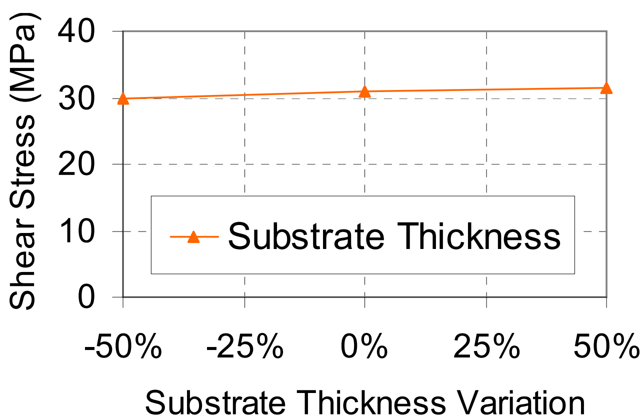

Figure 18: Effect of substrate thickness on the total shear stress.

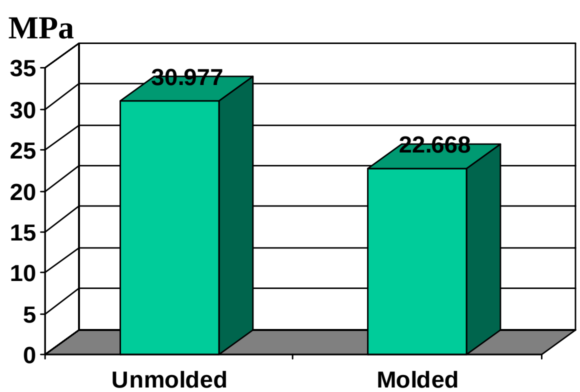

Figure 19: Effect of overmold on the total shear stress of NFU.

6. Conclusion

The package robustness of a larger die, copper pillar bump flip chip package with no-flow underfill has been evaluated. Comprehensive thermo-mechanical and hygroswelling models are established to study the package with no flow underfill during reflow after moisture preconditioning. The actual failure mechanism is complex, contributed by combined effects of process defects, interfacial adhesion strength, thermal stress and hygroswelling stress. From modeling, the maximum total shear stress location correlates well with the reliability test results.

A series of parametric studies have also been performed to eliminate/reduce the fillet crack. The results show that lower CTE & E of no-flow underfill and higher cure temperature of no-flow underfill are desirable for the robustness of the package. The results also show that thinner die thickness is desirable the robustness of the package. These findings form design guidelines for the design of the larger die, copper pillar bump flip chip package with no-flow underfill.

Acknowledgements

This work is the result of a project initiated by IME and APS. The authors would like to thank EDB, Singapore and A*STAR for the management support and financial support through T-UP program. The authors are grateful to the APS staff members who helped to realize this work, especially, Mr. HK Tan, Mr. KK Lau, Mr. Chng Han Shen and Mr. Ivan Wong. Appreciation is also extended to IME personnel who helped to realize this work, especially, Mr. Tan Teck Chun, Dr. M. K. Iyer, Mr. Chai Tai Chong and Dr. Lim Thiam Beng.

References

[1] The National Technology Roadmap for Semiconductors: Technology Needs. Semiconductor Industry Association, 1997.

[2] Schubert A, Dudek R, Leutenbauer R, Coskina P, Becker KF, Kloeser J, et al. Numerical and experimental investigations of large IC flip chip attach. In: Proc. 50th Electronic Components and Technology Conference, ECTC 2000, Las Vegas, NE, May 2000. p. 1338-1346.

[3] Hannemann R, Kraus AD, Pecht M. Semiconductor packaging: a multidisciplinary approach. New York: John Wiley & Sons, Inc., 1994.

[4] Goodelle JP, Amin A, Gilbert J, Horvath C, Nease E and Vaccaro BT. Large die flip chip packaging on organic substrate: the role of finite element analysis (FEA), materials characterization, failure analysis (FA) and test vehicles in development spins. In: Proc. 53rd Electronic Components and Technology Conference, ECTC 2003, New Orleans, LA, May 2003. p. 524-535.

[5] http://www.advanpack.com

[6] Wang T, Chew TH, Lum C, Chew YX, Miao P, Foo L. Assessment of flip chip assembly and reliability via reflowable underfill. In: Proc. 51st Electronic Components and Technology Conference, ECTC 2001, USA, 2001.

[7] Pecht M., Agarwal R, McCluskey P, Dishongh T, Javadpour S, Mahajan R. Electronic packaging materials and their properties. New York: CRC Press, Inc; 1998.

[8] Wong CP, Shi SH, Jefferson G. High performance no-flow underfills for low-cost flip-chip applications. In: Proc. 47th Electronic Components and Technology Conference, ECTC 1997, San Jose, CA, May, 1997, p. 850-858.

[9] Zhang Z and Wong CP. Assembly of lead-free bumped flip-chip with no-flow underfillls. IEEE Transactions on Electronics Packaging Manufacturing 2002; 25(2): 113-119.

[10] Ferguson TP, Qu J. Moisture absorption in no-flow underfill materials and its effect on interfacial adhesion to solder mask coated FR4 print wiring board. In: Proc. 2001 International Symposium on Advanced Packaging Materials, 2001. p. 327-332.

[11] Thorpe R, Baldwin DF, Smith B and McGovern L. Yield analysis and process modeling of low cost, high throughput flip chip assembly based on no-flow underfilll materials. IEEE Transactions on Electronics Packaging Manufacturing 2001; 24(2): 123-135.

[12] Tee TY, Kho CL, Yap D, Toh C, Baraton X, Zhong ZW. Reliability assessment and hygroswelling modeling of FCBGA with no-flow underfill. Microelectronics Reliability 2003; 43:741-749.

[13] Moon KS, Fan L, Wong CP. The effect toughening of no-flow underfill on fillet cracking of flip-chip device. In Proc. 2001 International Symposium on Advanced Packaging Materials, 2001. p. 333-340.

[14] Zhang X, Wong EH, Lee C, Chai TC, Ma Y, Teo PS, Pinjala D, Sampath S. Thermo-mechanical finite element analysis in a multi chip build up substrate based package design. Microelectronics Reliability 2004; 44:611-619.

[15] Lu J, Smith B, Baldwin DF. Adhesion characterization of no-flow underfillls used flip chip assemblies and correlation with reliability. IEEE Transactions on Electronics Packaging Manufacturing 2001; 24(1):26-30.

[16] Lau JH, Chang C, Chen CC. Characteristics and reliability of no-flow underfills for solder bumped flip chip assemblies. Intl. Journal of Microcircuits and Electronic Packaging 1999; 22(4): 370-381.

[17] Zhang X, Wong EH, Rajoo R, Iyer MK, Caers JFJM, Zhao XJ. Development of process modeling methodology for flip chip on flex interconnections with non-conductive adhesives. Microelectronics Reliability 2005; 45:1215-1221.

[18] Wong EH., Chan KC, Rajoo R., Lim TB. The mechanics and impact of hygroscopic swelling of polymeric materials in electronic packages. In: Proc. 50th Electronic Component Technology Conference, ECTC, Las Vegas, NE, USA, May 2000. p. 576-580.